

Article

Modification of Deposited, Size-Selected MoS₂ Nanoclusters by Sulphur Addition: An Aberration-Corrected STEM Study

Yubiao Niu, Sung Jin Park and Richard E. Palmer *

Nanoscale Physics, Chemistry and Engineering Research Laboratory, School of Physics & Astronomy, University of Birmingham, Birmingham B15 2TT, UK; y.niu@bham.ac.uk (Y.N.); s.j.park@bham.ac.uk (S.J.P.)

* Correspondence: R.E.Palmer@bham.ac.uk; Tel.: +44-0121-414-4653

Academic Editors: Stefan T. Bromley and Scott M. Woodley

Received: 28 October 2016; Accepted: 20 December 2016; Published: 22 December 2016

Abstract: Molybdenum disulphide (MoS₂) is an earth-abundant material which has several industrial applications and is considered a candidate for platinum replacement in electrochemistry. Size-selected MoS₂ nanoclusters were synthesised in the gas phase using a magnetron sputtering, gas condensation cluster beam source with a lateral time-of-flight mass selector. Most of the deposited MoS₂ nanoclusters, analysed by an aberration-corrected scanning transmission electron microscope (STEM) in high-angle annular dark field (HAADF) mode, showed poorly ordered layer structures with an average diameter of 5.5 nm. By annealing and the addition of sulphur to the clusters (by sublimation) in the cluster source, the clusters were transformed into larger, crystalline structures. Annealing alone did not lead to crystallization, only to a cluster size increase by decomposition and coalescence of the primary clusters. Sulphur addition alone led to a partially crystalline structure without a significant change in the size. Thus, both annealing and sulphur addition processes were needed to obtain highly crystalline MoS₂ nanoclusters.

Keywords: molybdenum disulphide; MoS₂; STEM; cluster; crystalline; sulphur addition

1. Introduction

Two-dimensional transition metal dichalcogenides (TMD) have attracted renewed attention since the isolation of graphene [1–3]. Molybdenum disulphide (MoS₂), as a representative member of the TMD family, has been widely investigated because of its intriguing catalytic [4,5], electronic [6–8], optoelectronic [9], and tribological [10] properties. MoS₂ layers have a sandwich structure with molybdenum atoms arranged between two sulphur sheets [7,11,12]. In nanoparticles, the atoms at the edge sites of the MoS₂ layers, rather than the basal plane atoms, make the main contribution to the catalytic activity. An example is the hydrogen evolution reaction (HER), where low-coordinated, additional sulphur atoms at Mo-edge sites are notably active in HER [4,13–15]. In this case the material is sulphur-rich, with a stoichiometry of MoS_{2+x}, rather than MoS₂. The electrocatalytic activity tends to decrease with an increase in the number of MoS₂ layers, due to poor electron hopping efficiency between the stacked layers [16]. In general, edge-abundant MoS₂ nanomaterials remain a potential substitute for scarce and costly platinum-based catalysts [15,17]. Good control over the atomic structure of MoS₂ nanostructures should contribute to the enhancement of the catalytic performance.

Several methods have been developed to fabricate nanostructured MoS₂ with one or several layers, such as chemical exfoliation of bulk MoS₂ [18], chemical vapor deposition (CVD) [16,19] and solvothermal synthesis [20]. However, the chemical preparation of MoS₂ nanomaterials with well-defined size is still a formidable challenge. The preparation of size-selected MoS₂ nanoclusters by the cluster beam deposition technique was reported by Cuddy et al. [5]. The clusters were reported to

be somewhat sulphur-poor. Sulphur addition by an electrochemical method was reported recently [21]. Here we report an in-vacuum processing approach, based on a combination of sulphur addition (by sublimation) and annealing inside the cluster beam source, to increase the sulphur content of the clusters and to explore structural modifications. The atomic structures of these MoS₂ clusters were characterised with an aberration-corrected scanning transmission electron microscope (STEM) in high-angle annular dark field (HAADF) mode [22–25]. The modification process leads to enhanced cluster crystallinity at the cost of some increase in the cluster size.

2. Results and Discussion

MoS₂ nanoclusters with a mass of 160,000 amu, corresponding nominally to (MoS₂)₁₀₀₀, were produced using a gas condensation, magnetron sputtering cluster source in conjunction with a lateral time-of-flight mass filter [26,27]. The clusters were deposited onto amorphous carbon-covered TEM grids with an impact energy of 1.5 eV per MoS₂ unit. Figure 1a shows an aberration-corrected HAADF-STEM image of (MoS₂)₁₀₀₀ clusters at low magnification with a peak diameter of 5.5 nm (Figure 1b). The clusters were deposited with a surface coverage of ~5% to keep them separate. However, the image shows that some clusters diffused and aggregated after deposition. The HAADF intensity distribution (Figure 1c) measured from 155 independent clusters indicates several peaks in the size spectrum. In order to confirm which peak corresponds to the original (MoS₂)₁₀₀₀ clusters, the size of the cluster shown in Figure 1d was derived from Mo atom counting [22,28]. This cluster was found to contain approximately 1100 Mo atoms and is located in peak 3. This indicates peak 3 is the peak corresponding to the original (MoS₂)₁₀₀₀ clusters, while peak 4 corresponds to clusters with double mass. We note there are some clusters located in the lower intensity region (peaks 1 and 2, Figure 1c) and, correspondingly, in the smaller diameter region (3.8 ± 1.8 nm, Figure 1b). We believe that these smaller clusters may come from the fragmentation of the original clusters during the impact on the substrate surface. It is notable that the sum of the peak intensities of peak 1 and peak 2 in Figure 1c is located in the region of peak 3. An interpretation is that, during the formation process in the cluster source, small clusters may sometimes aggregate, being bonded to each other with a rather weak interaction in the gas condensation process. We envisage that such “composite clusters” may break up into two or more smaller clusters when they land on the support.

Figure 1d highlights the atomic structure of one MoS₂ cluster at higher magnification and includes a fast Fourier transform (FFT) pattern (inset). The shape of the cluster is rather irregular and the absence of extended crystalline order is confirmed by the diffuse ring in the FFT pattern. While most clusters present such poorly ordered structures, a few clusters are observed with a more developed crystalline structure, as shown in Figure 1f. The uneven-layered structure of the cluster is evident in the steps in the HAADF intensity line profile (Figure 1e). The STEM image intensity is proportional to the number of MoS₂ layers. The HAADF intensity line profile indicates the cluster has an approximate pyramid shape with four layers in the central part. The layered structure of the MoS₂ clusters is also confirmed by the side-on cluster shown in Figure 1g. This side-on structure displays the (002) edge sites with a 0.67 nm interlayer spacing comparable with that of bulk MoS₂ (0.65 nm) [29]. Similar TEM images of particular side-on MoS₂ nanoparticles were reported recently by Fei et al. [30]. Such side-on clusters were captured in only a few cases, which might depend on favourable bonding to particular defects on the support.

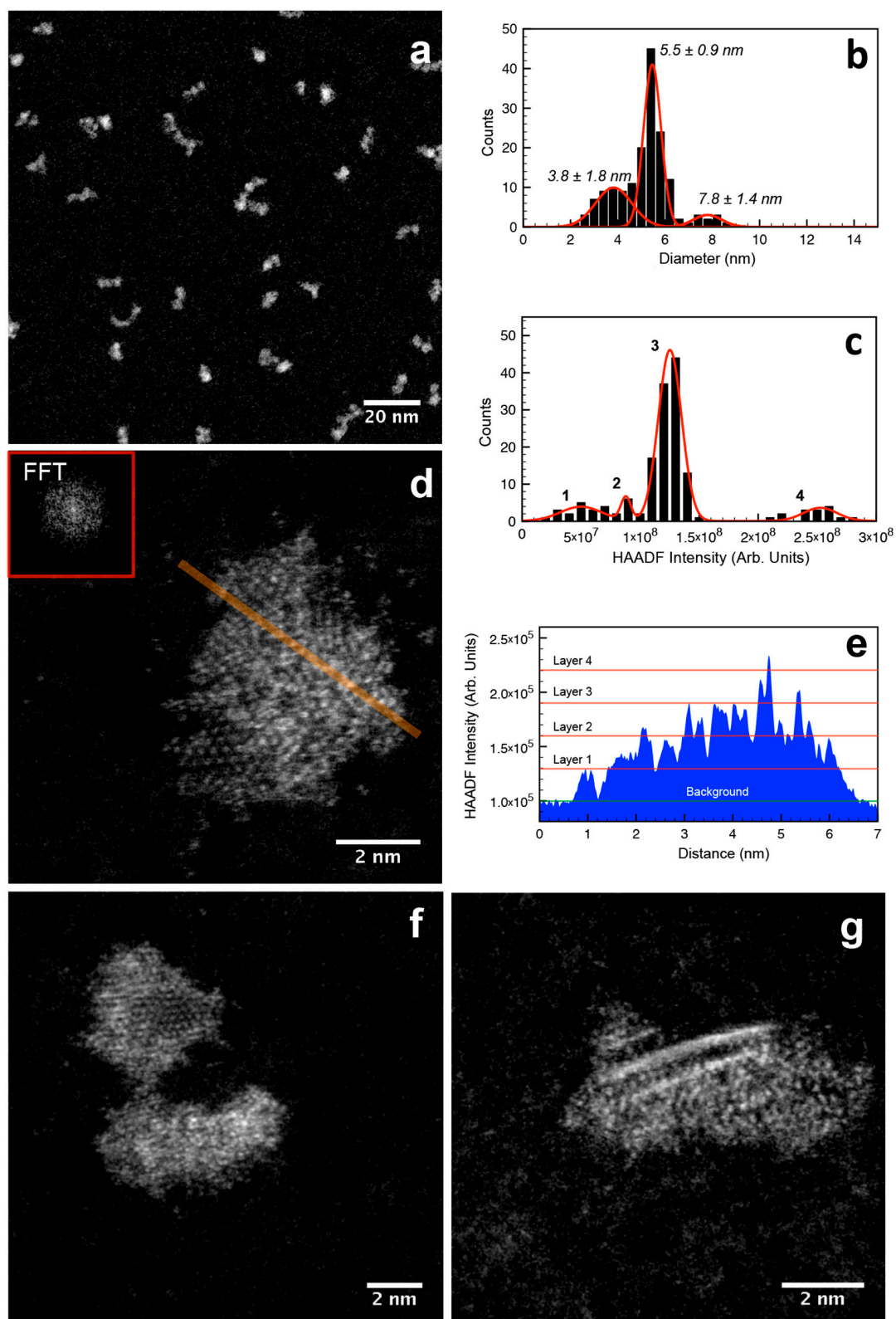


Figure 1. STEM images of as-deposited, size-selected $(\text{MoS}_2)_{1000}$ clusters shown at (a) low and (d) high magnification with FFT pattern inset; (b) Size distribution and (c) integrated HAADF intensity distribution of independent clusters; (e) HAADF intensity line profile corresponding to the orange line in (d); (f) $(\text{MoS}_2)_{1000}$ cluster with partially crystalline structure; (g) A side-on (oriented perpendicular to the substrate) MoS_2 cluster displays its layered structure.

The previous study of MoS₂ clusters by Cuddy et al. [5] from our group demonstrated that the as-deposited MoS₂ nanoclusters were sulphur-deficient; the X-ray photoelectron spectroscopy (XPS) measurement gave a Mo:S ratio of 1:(1.6 ± 0.1) rather than 1:2. One possible cause of the limited crystallinity of the as-deposited MoS₂ nanoclusters observed here is such a sulphur deficiency. Thus, we have explored the addition of sulphur (by thermal sublimation of solid sulphur for 5 min) to the deposited clusters, in vacuum (in the cluster source), accompanied by thermal annealing (7 min, 215 ± 5 °C). The nominal amount of sulphur deposited was equivalent to a thick film (10,000 layers) but the excess sulphur (i.e., beyond that which bonds chemically to the clusters) should be sublimed away from the cluster surface given the annealing temperature. Sulphur has long been known to sublime at temperatures well below 100 °C [31,32]. The STEM images and HAADF intensities of clusters subjected to this additional treatment are presented in Figure 2. Compared with the as-deposited clusters (Figure 1a), the STEM image at low magnification (Figure 2a) reveals that the “sulphurised” and annealed clusters became larger. The size distribution shown in Figure 2b gives a peak diameter of 6.0 nm. The fragmental clusters (3.8 nm, Figure 1b) may recombine with each other in this treatment, leading to the absence of the peak of smaller size in Figure 2b. STEM images at high magnification indicate that most of the clusters have rather crystalline structures. Figure 2c shows a single crystalline MoS₂ cluster with a single set of diffraction spots corresponding to the (100) plane with 0.26 nm spacing. The regular honeycomb pattern shown here originates from the atomic arrangements of Mo and S atoms, which is in agreement with the TEM studies on the MoS₂ nanoparticles made by other methods, e.g., CVD and exfoliation [33,34]. The intensity profile shows this cluster consists of two, non-identical hexagonal layers; the brighter region in the middle has a bi-layered structure with mono-layer structures on both sides. While some clusters present this kind of layer stacking with the hexagonal atomic structure, some clusters show misorientation between layers, leading to a Moiré pattern. The cluster shown in Figure 2d consists of four layers; the layer step changes can be seen in the STEM image and are confirmed by the HAADF intensity line profile shown in Figure 2e. Layer 2 has a ~30° rotation angle with respect to layer 1, which is indicated by the STEM image and the two sets of diffraction spots in the FFT pattern. As in the case of as-deposited samples, we found a minority of side-on MoS₂ cluster structures after sulphur addition and annealing (Figure 2f). This suggests that sulfur deficiency does not deteriorate the layered nature of MoS₂, in agreement with the simulation first-principles study done by Wu et al. [35], and sulphur addition and annealing do not affect the layer arrangement of the clusters and that the structural modification into crystalline clusters mainly takes place within the 2D layers.

To further understand the effect of the combined sulphur addition and annealing treatment on the MoS₂ cluster structures, we independently treated as-deposited MoS₂ clusters by annealing or sulphur addition alone. Annealed clusters are illustrated in Figure 3a,b, where the clusters present poorly ordered structures confirmed by the diffuse FFT pattern. The most notable change is in the cluster size, which now shows two main peaks at 3.1 nm and 8.9 nm in the size distribution, shown in Figure 3c. Thus, the 5.5 nm peak in the original size distribution (Figure 1b) disappeared. As discussed above, some of the as-deposited (MoS₂)₁₀₀₀ clusters are actually the result of the weak binding of several smaller clusters in the gas phase. We envisage that these component clusters are liberated in the annealing process, leading to the 3.1 nm peak in Figure 3c, or migrating and coalescing with other clusters to generate the 8.9 nm peak. Such a process could account for the dissolution of the main peak in Figure 1b and the formation of the two new main peaks in Figure 3c.

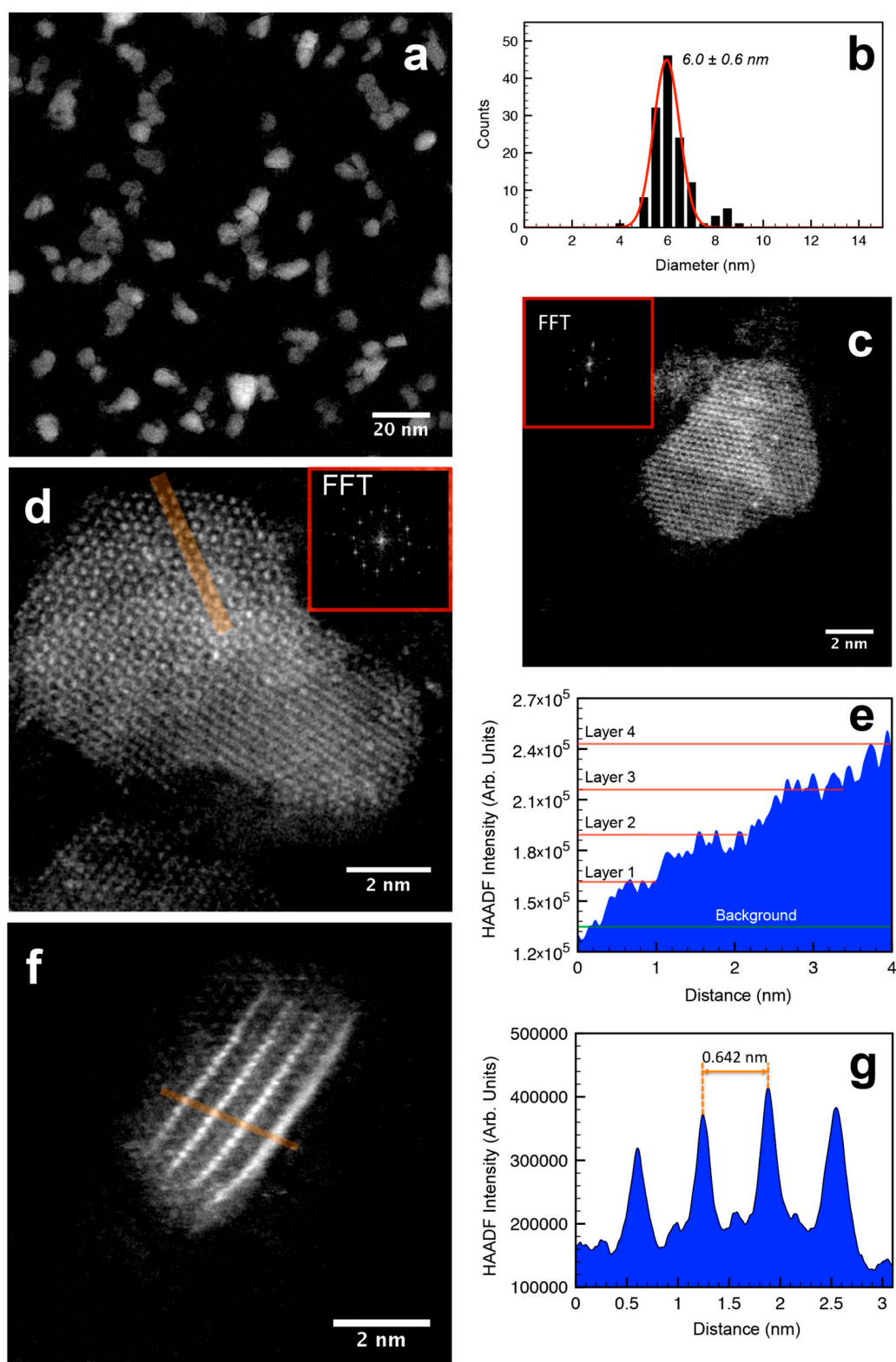


Figure 2. STEM images of (a) (MoS₂)₁₀₀₀ clusters with sulphur addition and annealing at low magnification; (b) Size distribution of independent clusters; (c) Bi-layered MoS₂ cluster with FFT pattern; (d) MoS₂ cluster with four layers with FFT pattern, indicating a ~30° rotation angle between first (from bottom) and second layer; (e) HAADF intensity line profile of the line in (d); (f) A side-on MoS₂ cluster with a 0.64 nm interlayer spacing and (g) its HAADF intensity line profile of the line in (e).

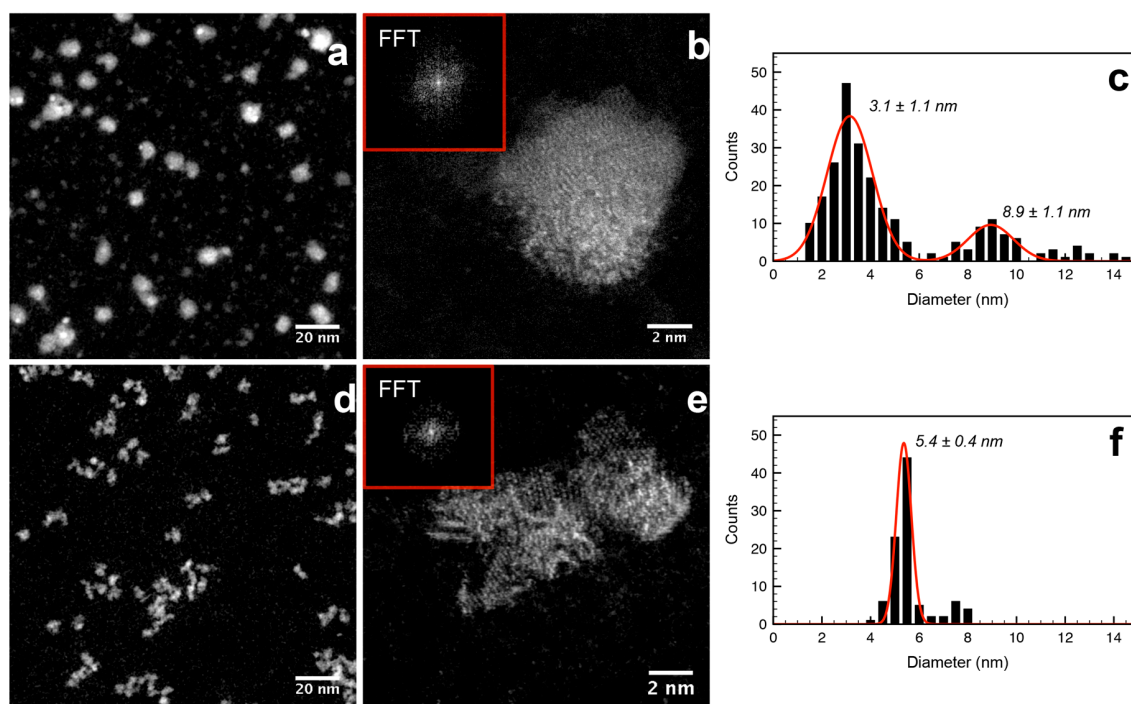


Figure 3. STEM images of MoS₂ clusters after (a,b) annealing only and (d,e) after sulphur addition only of as-deposited samples, (MoS₂)₁₀₀₀; (c,f) are the corresponding size distributions of the clusters after annealing only and sulphur addition only, respectively.

In contrast with annealing, surface diffusion of clusters and coalescence is rarely observed in the purely sulphurised samples shown in Figure 3d. Their size distribution is illustrated in Figure 3f, showing a similar peak diameter (5.4 nm) as the as-deposited sample (5.5 nm, Figure 1b). Note that there is no evidence in the images of a thick film of sulphur on the clusters; we suspect that warming of the sample by radiation from the nearby evaporator is sufficient to induce re-sublimation. These sulphurised MoS₂ clusters (Figure 3e) show a partial improvement in crystalline structure, unlike the annealed MoS₂ samples, but not to the same extent as the clusters which are both sulphurised and annealed. We concluded that the combination of annealing and sulphur addition of as-deposited, amorphous MoS₂ nanoclusters is the best way to create the extended crystalline structures.

It has been reported that the structural damage on a crystalline MoS₂ structure could be induced by an electron beam, where the maximum transferred energy from an electron beam with 200 kV is larger than the displacement threshold energy of the sulphur atom [36]. However, significant damage on the MoS₂ crystalline structure was hardly observed in this work. This is presumably because of a short exposure time to the electron beam during taking images (~20 s for each image) and a small number of MoS₂ layers. Although we cannot rule out the possibility of the electron beam damaging the structure, it does not affect the conclusion of this work.

In summary, we have modified size-selected (MoS₂)₁₀₀₀ clusters, generated with a gas condensation cluster beam source and mass filter, by additional treatments after deposition. The aberration-corrected STEM images reveal layered but poorly crystalline features for most as-deposited clusters. However, a combination of sulphur addition and annealing led to a notable increase in extended crystallinity and a moderate increase in size. Clusters show decomposition and coalescence, resulting in both larger and smaller sizes compared with the as-deposited samples, whereas the clusters simply sulphurised retain their size but are only partially crystallised. Thus, to obtain the most crystalline MoS₂ nanoclusters, the combination of annealing and sulphur addition is needed. This method, once developed further, may offer a new route to the creation of well-defined MoS₂ clusters with a few layers for catalytic use.

3. Materials and Methods

Size-selected MoS₂ nanoclusters were produced using a magnetron sputtering (DC, 45 W) and gas condensation cluster beam source [27]. A 2-inch sputtering MoS₂ target (PI-KEM, Tamworth, UK, 99.9% purity) was used and Ar (180 sccm) and He (160 sccm) gases were introduced to enable sputtering and cluster condensation, respectively. The positively charged clusters were accelerated with ion optical electrostatic lenses and then size-selected with a lateral time-of-flight mass filter [26]. A mass of 160,000 amu, corresponding to (MoS₂)₁₀₀₀, was selected for depositing onto an amorphous carbon coated TEM grids (Agar Scientific, Stansted, UK, 200 Mesh Cu). Sulphur addition was conducted in a sulphur atmosphere created by evaporating sulphur using a home-built in-situ thermal evaporator (5 min). Annealing (7 min, 215 ± 5 °C) was performed with an electron beam bombardment heating stage. The temperature was monitored using a pyrometer (IMPAC Pyrometer, IPE 140, LumaSense Technologies GmbH, Frankfurt, Germany). All the STEM images were taken with a 200 kV spherical aberration-corrected STEM (JEOL 2100F, Tokyo, Japan) in the HAADF mode [22–25].

Acknowledgments: The authors acknowledge the financial support from the European Research Council Marie-Curie ITN “CATSENSE”.

Author Contributions: The manuscript was written through contributions of Yubiao Niu, Sung Jin Park and Richard E. Palmer. Yubiao Niu, Sung Jin Park and Richard E. Palmer have given approval to the final version of the manuscript.

Conflicts of Interest: The authors declare no conflict of interest.

References

1. Novoselov, K.S.; Jiang, D.; Schedin, F.; Booth, T.J.; Khotkevich, V.V.; Morozov, S.V.; Geim, A.K. Two-dimensional atomic crystals. *Proc. Natl. Acad. Sci. USA* **2005**, *102*, 10451–10453. [[CrossRef](#)] [[PubMed](#)]
2. Chhowalla, M.; Shin, H.S.; Eda, G.; Li, L.J.; Loh, K.P.; Zhang, H. The chemistry of two-dimensional layered transition metal dichalcogenide nanosheets. *Nat. Chem.* **2013**, *5*, 263–275. [[CrossRef](#)] [[PubMed](#)]
3. Akinwande, D.; Petrone, N.; Hone, J. Two-dimensional flexible nanoelectronics. *Nat. Commun.* **2014**, *5*. [[CrossRef](#)] [[PubMed](#)]
4. Gemming, S.; Seifert, G. Nanocrystals: Catalysts on the edge. *Nat. Nanotechnol.* **2007**, *2*, 21–22. [[CrossRef](#)] [[PubMed](#)]
5. Cuddy, M.J.; Arkill, K.P.; Wang, Z.W.; Komsa, H.P.; Krashennnikov, A.V.; Palmer, R.E. Fabrication and atomic structure of size-selected, layered MoS₂ clusters for catalysis. *Nanoscale* **2014**, *6*, 12463–12469. [[CrossRef](#)] [[PubMed](#)]
6. Wu, W.; Wang, L.; Li, Y.; Zhang, F.; Lin, L.; Niu, S.; Chenet, D.; Zhang, X.; Hao, Y.; Heinz, T.F.; et al. Piezoelectricity of single-atomic-layer MoS₂ for energy conversion and piezotronics. *Nature* **2014**, *514*, 470–474. [[CrossRef](#)] [[PubMed](#)]
7. Ganatra, R.; Zhang, Q. Few-layer MoS₂: A promising layered semiconductor. *ACS Nano* **2014**, *8*, 4074–4099. [[CrossRef](#)] [[PubMed](#)]
8. Laursen, A.B.; Kegnaes, S.; Dahl, S.; Chorkendorff, I. Molybdenum sulfides—Efficient and viable materials for electro- and photoelectrocatalytic hydrogen evolution. *Energy Environ. Sci.* **2012**, *5*, 5577–5591. [[CrossRef](#)]
9. Wang, Q.H.; Kalantar-Zadeh, K.; Kis, A.; Coleman, J.N.; Strano, M.S. Electronics and optoelectronics of two-dimensional transition metal dichalcogenides. *Nat. Nanotechnol.* **2012**, *7*, 699–712. [[CrossRef](#)] [[PubMed](#)]
10. Chen, Z.; Liu, X.; Liu, Y.; Gunsel, S.; Luo, J. Ultrathin MoS₂ Nanosheets with Superior Extreme Pressure Property as Boundary Lubricants. *Sci. Rep.* **2015**, *5*. [[CrossRef](#)] [[PubMed](#)]
11. Yang, D.; Sandoval, S.; Divigalpitiya, W.; Irwin, J.; Frindt, R. Structure of single-molecular-layer MoS₂. *Phys. Rev. B* **1991**, *43*, 12053–12056. [[CrossRef](#)]
12. Joswig, J.O.; Lorenz, T.; Wendumu, T.B.; Gemming, S.; Seifert, G. Optics, mechanics, and energetics of two-dimensional MoS₂ nanostructures from a theoretical perspective. *Acc. Chem. Res.* **2015**, *48*, 48–55. [[CrossRef](#)] [[PubMed](#)]
13. Jaramillo, T.F.; Jorgensen, K.P.; Bonde, J.; Nielsen, J.H.; Horch, S.; Chorkendorff, I. Identification of active edge sites for electrochemical H₂ evolution from MoS₂ nanocatalysts. *Science* **2007**, *317*, 100–102. [[CrossRef](#)] [[PubMed](#)]

14. Kibsgaard, J.; Jaramillo, T.F.; Besenbacher, F. Building an appropriate active-site motif into a hydrogen-evolution catalyst with thiomolybdate $[\text{Mo}_3\text{S}_{13}]^{2-}$ clusters. *Nat. Chem.* **2014**, *6*, 248–253. [[CrossRef](#)] [[PubMed](#)]
15. Hinnemann, B.; Moses, P.G.; Bonde, J.; Jorgensen, K.P.; Nielsen, J.H.; Horch, S.; Chorkendorff, I.; Norskov, J.K. Biomimetic hydrogen evolution: MoS_2 nanoparticles as catalyst for hydrogen evolution. *J. Am. Chem. Soc.* **2005**, *127*, 5308–5309. [[CrossRef](#)] [[PubMed](#)]
16. Yu, Y.; Huang, S.Y.; Li, Y.; Steinmann, S.N.; Yang, W.; Cao, L. Layer-dependent electrocatalysis of MoS_2 for hydrogen evolution. *Nano Lett.* **2014**, *14*, 553–558. [[CrossRef](#)] [[PubMed](#)]
17. Karunadasa, H.I.; Montalvo, E.; Sun, Y.J.; Majda, M.; Long, J.R.; Chang, C.J. A Molecular MoS_2 Edge Site Mimic for Catalytic Hydrogen Generation. *Science* **2012**, *335*, 698–702. [[CrossRef](#)] [[PubMed](#)]
18. Wang, T.Y.; Liu, L.; Zhu, Z.W.; Papakonstantinou, P.; Hu, J.B.; Liu, H.Y.; Li, M.X. Enhanced electrocatalytic activity for hydrogen evolution reaction from self-assembled monodispersed molybdenum sulfide nanoparticles on an Au electrode. *Energy Environ. Sci.* **2013**, *6*, 625–633. [[CrossRef](#)]
19. Van der Zande, A.M.; Huang, P.Y.; Chenet, D.A.; Berkelbach, T.C.; You, Y.; Lee, G.H.; Heinz, T.F.; Reichman, D.R.; Muller, D.A.; Hone, J.C. Grains and grain boundaries in highly crystalline monolayer molybdenum disulphide. *Nat. Mater.* **2013**, *12*, 554–561. [[CrossRef](#)] [[PubMed](#)]
20. Xie, J.F.; Zhang, H.; Li, S.; Wang, R.X.; Sun, X.; Zhou, M.; Zhou, J.F.; Lou, X.W.; Xie, Y. Defect-Rich MoS_2 Ultrathin Nanosheets with Additional Active Edge Sites for Enhanced Electrocatalytic Hydrogen Evolution. *Adv. Mater.* **2013**, *25*, 5807–5813. [[CrossRef](#)] [[PubMed](#)]
21. Burch, H.A.; Isaacs, M.; Wilson, K.; Palmer, R.E.; Rees, N.V. Electrocatalytic regeneration of atmospherically aged MoS_2 nanostructures via solution-phase sulfidation. *RSC Adv.* **2016**, *6*, 26689–26695. [[CrossRef](#)]
22. Wang, Z.W.; Toikkanen, O.; Yin, F.; Li, Z.Y.; Quinn, B.M.; Palmer, R.E. Counting the atoms in supported, monolayer-protected gold clusters. *J. Am. Chem. Soc.* **2010**, *132*, 2854–2855. [[CrossRef](#)] [[PubMed](#)]
23. Wang, Z.W.; Palmer, R.E. Determination of the Ground-State Atomic Structures of Size-Selected Au Nanoclusters by Electron-Beam-Induced Transformation. *Phys. Rev. Lett.* **2012**, *108*. [[CrossRef](#)] [[PubMed](#)]
24. Jian, N.; Palmer, R.E. Variation of the Core Atomic Structure of Thiolated $(\text{Au}_x\text{Ag}_{1-x})_{312\pm 55}$ Nanoclusters with Composition from Aberration-Corrected HAADF STEM. *J. Phys. Chem. C* **2015**, *119*, 11114–11119. [[CrossRef](#)]
25. Jian, N.; Stapelfeldt, C.; Hu, K.J.; Froba, M.; Palmer, R.E. Hybrid atomic structure of the Schmid cluster $\text{Au}_{55}(\text{PPh}_3)_{12}\text{Cl}_6$ resolved by aberration-corrected STEM. *Nanoscale* **2015**, *7*, 885–888. [[CrossRef](#)] [[PubMed](#)]
26. Von Issendorff, B.; Palmer, R.E. A new high transmission infinite range mass selector for cluster and nanoparticle beams. *Rev. Sci. Instrum.* **1999**, *70*, 4497–4501. [[CrossRef](#)]
27. Pratontep, S.; Carroll, S.J.; Xirouchaki, C.; Streun, M.; Palmer, R.E. Size-selected cluster beam source based on radio frequency magnetron plasma sputtering and gas condensation. *Rev. Sci. Instrum.* **2005**, *76*. [[CrossRef](#)]
28. Escalera-López, D.; Niu, Y.; Yin, J.; Cooke, K.; Rees, N.V.; Palmer, R.E. Enhancement of the Hydrogen Evolution Reaction from Ni- MoS_2 Hybrid Nanoclusters. *ACS Catal.* **2016**, *6*, 6008–6017. [[CrossRef](#)] [[PubMed](#)]
29. Shi, Y.; Zhou, W.; Lu, A.Y.; Fang, W.; Lee, Y.H.; Hsu, A.L.; Kim, S.M.; Kim, K.K.; Yang, H.Y.; Li, L.J.; et al. van der Waals epitaxy of MoS_2 layers using graphene as growth templates. *Nano Lett.* **2012**, *12*, 2784–2791. [[CrossRef](#)] [[PubMed](#)]
30. Fei, L.; Lei, S.; Zhang, W.B.; Lu, W.; Lin, Z.; Lam, C.H.; Chai, Y.; Wang, Y. Direct TEM observations of growth mechanisms of two-dimensional MoS_2 flakes. *Nat. Commun.* **2016**, *7*. [[CrossRef](#)] [[PubMed](#)]
31. Tucker, R.P. Notes on the sublimation of sulfur between 25° and 50 °C. *Ind. Eng. Chem.* **1929**, *21*, 44–47. [[CrossRef](#)]
32. Grugel, R.N.; Toutanji, H. Sulfur “concrete” for lunar applications—Sublimation concerns. *Adv. Space Res.* **2008**, *41*, 103–112. [[CrossRef](#)]
33. Ji, Q.; Zhang, Y.; Gao, T.; Zhang, Y.; Ma, D.; Liu, M.; Chen, Y.; Qiao, X.; Tan, P.H.; Kan, M.; et al. Epitaxial monolayer MoS_2 on mica with novel photoluminescence. *Nano Lett.* **2013**, *13*, 3870–3877. [[CrossRef](#)] [[PubMed](#)]
34. Muscuso, L.; Cravanzola, S.; Cesano, F.; Scarano, D.; Zecchina, A. Optical, Vibrational, and Structural Properties of MoS_2 Nanoparticles Obtained by Exfoliation and Fragmentation via Ultrasound Cavitation in Isopropyl Alcohol. *J. Phys. Chem. C* **2015**, *119*, 3791–3801. [[CrossRef](#)]

35. Wu, Z.; Wang, Y.; Ye, Y.; Feng, J.; Zhang, M.; Luo, Y.; He, L.; Cao, W. First-principles study of monolayer MoS₂ with deficient and excessive Mo_n and S_n ($n = -3 \rightarrow 3$) clusters on 5×5 supercells. *Comput. Mater. Sci.* **2016**, *121*, 124–130. [[CrossRef](#)]
36. Garcia, A.; Raya, A.M.; Mariscal, M.M.; Esparza, R.; Herrera, M.; Molina, S.I.; Scavello, G.; Galindo, P.L.; Jose-Yacamán, M.; Ponce, A. Analysis of electron beam damage of exfoliated MoS₂ sheets and quantitative HAADF-STEM imaging. *Ultramicroscopy* **2014**, *146*, 33–38. [[CrossRef](#)] [[PubMed](#)]



© 2016 by the authors; licensee MDPI, Basel, Switzerland. This article is an open access article distributed under the terms and conditions of the Creative Commons Attribution (CC-BY) license (<http://creativecommons.org/licenses/by/4.0/>).